Published OnlineFirst January 22, 2014; DOI: 10.1158/0008-5472.CAN-13-1446

Chromosome 10, Frequently Lost in Human Melanoma, Encodes Multiple Tumor-Suppressive Functions

Lawrence N. Kwong and Lynda Chin

Abstract

Although many DNA aberrations in melanoma have been well characterized, including focal amplification and deletions of oncogenes and tumor suppressors, broad regions of chromosomal gain and loss are less well understood. One possibility is that these broad events are a consequence of collateral damage from targeting single loci. Another possibility is that the loss of large regions permits the simultaneous repression of multiple tumor suppressors by broadly decreasing the resident gene dosage and expression. Here, we test this hypothesis in a targeted fashion using RNA interference to suppress multiple candidate residents in broad regions of loss. We find that loss of chromosome regions 6q, 10, and 11q21-ter is correlated with broadly decreased expression of most resident genes and that multiple resident genes impacted by broad regional loss of chromosome 10 are tumor suppressors capable of affecting tumor growth and/or invasion. We also provide additional functional support for Ablim1 as a novel tumor suppressor. Our results support the hypothesis that multiple cancer genes are targeted by regional chromosome copy number aberrations. *Cancer Res; 74(6); 1814–21. ©2014 AACR.*

Introduction

Increasingly high-resolution genomic studies have established that recurrent focal deletions and amplifications in cancer can selectively target specific oncogenes and tumor suppressors (1, 2). In melanoma, *MITF, CCND1, BRAF, CDKN2A*, and *PTEN* are some of the validated oncogenes and tumor suppressors targeted by such focal copy number-changing aberrations (3–5). However, there are also many recurrent large regional or arm-level losses and gains that affect multiple resident genes (6, 7). One hypothesis states that most of these represent bystander passengers deleted or gained coincidentally along with the driver genes. However, increasing evidence is pointing toward the presence of multiple cancer driver genes targeted by these regional alterations. Recent papers have described multiple tumor growth suppressors in broad regions of loss, in an *in vitro* genome-wide assay (8) and in a targeted *in vivo* screen of chromosome 8 for liver cancer (9).

In melanoma, loss of the entire chromosome 10 was identified as early as 1991 (10). On the basis of focal deletions at 10q23.3 and the presence of loss-of-function mutations, *PTEN* was functionally validated as the genetic target of the loss (11, 12). However, focal inactivation of *PTEN* is seen in only approximately 10% of melanomas, whereas copy number loss of the entire chromosome 10 is observed in >50% of melanomas (7). In contrast, the observed approximately 60% of *CDKN2A/B* deletions on chromosome 9p are focal. These data suggest that although *PTEN* is a major driver of chromosome 10 loss, other genes may also be targeted for inactivation. Here, we ask whether recurrent losses on human chromosomes 6, 10, and 11 in melanoma may broadly target multiple tumor suppressors acting at different steps in tumor progression.

Authors' Affiliation: Department of Genomic Medicine, University of Texas MD Anderson Cancer Center, Houston, Texas

Note: Supplementary data for this article are available at Cancer Research Online (http://cancerres.aacrjournals.org/).

Corresponding Author: Lynda Chin, MD Anderson Cancer Center, 1515 Holcombe Blvd. Unit 0091. Houston, TX 77030. Phone: 713-792-6876; Fax: 713-92-6806; E-mail: lchin@mdanderson.org

doi: 10.1158/0008-5472.CAN-13-1446

Materials and Methods

Determination of the 48 candidate genes

We previously published microarray expression data containing nine nevi, 25 primary melanomas, and 63 metastatic melanomas (6), which are now available publically on the Gene Expression Omnibus (http://www.ncbi.nlm.nih.gov/geo/), accession number GSE46517. We first generated a list of 144 genes that are significantly downregulated in the metastases compared with either the primary melanomas or nevi, based on the following criteria: $P < 0.05$, Student t test; >1.3-fold average decrease in expression; and >50% present calls in the primary melanoma or nevi group (13). We then intersected this list with an identical analysis of the data from Talantov and colleagues (14) and Riker and colleagues (15). On the basis of the publicly available probe data at the time of analysis, a total of 62 annotated genes were in common between our data and at least one of the other lists. Five genes were removed because of poor or no homology between human and mouse (*AKR1C1, AKR1C2, AKR1C3, C10orf116*, and *P53AIP1*). Of the remaining 57 genes, pLKO-based short hairpin RNAs (shRNA) were available for 48 (Supplementary Fig. S2).

Cell culture

The establishment and maintenance of iNRAS cell lines have been previously described (16). MUM2C, WM115, SKMel28, and 1205Lu human cell lines were maintained as mycoplasma-free

Published OnlineFirst January 22, 2014; DOI: 10.1158/0008-5472.CAN-13-1446

cultures in RPMI, 10% FBS. The MMM-7.1 primary melanocyte culture was initially isolated from 2-day-old FVB.CDKN2A$^{-/-}$ pups as previously described (17). Low-passage cultures were simultaneously retrovirally infected with a pBabe-hygro-BRAF^{V600E} and a pRetroSuper-shPten construct (18) and selected with hygromycin and puromycin. MMM-7.1 cultures were subsequently maintained in RPMI, 10% FBS, 200 nm 12-tetradecanoylphorbol 13-acetate (Sigma), and 200 pm cholera toxin (Sigma).

Mouse studies

Eight iNRAS cell lines were tested for *in vivo* tumor formation by intradermal injection of 5×10^5 cells into the flanks of nude mice (Taconic). All iNRAS cell lines require doxycycline to express oncogenic NRAS. All mice were therefore maintained on doxycycline chow (Harlan–Teklad). Two cell lines, iNRAS-463 and iNRAS-485, were selected for further use, based on their relatively long tumor latencies. For human xenografts, 1×10^6 cells were injected intradermally into the flanks of nude mice. For shRNA studies using the pTRIPZ-inducible vector, mice were maintained on doxycycline chow. For experimental lung metastasis assays, 5×10^5 B16F10 cells were injected into the tail vein of nude mice. Mice were sacrificed 15 days later and lung nodules were counted under a dissecting microscope. All animal experiments were performed according to protocols approved by the Institutional Animal Care and Use Committees at the Dana-Farber Cancer Institute (Boston, MA) and the University of Texas MD Anderson Cancer Center (Houston, TX).

In vivo shRNA screen

pLKO plasmid constructs targeting 48 genes were obtained as a generous gift from from Dr. William Hahn (Dana-Farber Cancer Center, Boston, MA). Four to five shRNAs were extracted and pooled per gene from equally mixed portions of bacteria using a Midiprep Kit (Qiagen). These were then further equally pooled according to chromosomal location (see Supplementary Fig. S2) before viral packaging and infection of iNRAS cell lines. All cells were transduced at a multiplicity of infection (MOI) of 0.5 without drug selection. After one day of recovery from the viral infection, cells from each pool were injected intradermally into both flanks of nude mice, using 5×10^5 cells per injection. Mice were monitored for tumor formation and tumor sizes were measured every 2 to 3 days. For secondary shRNA validation, individual or pooled shRNAs were packaged and transduced into the target iNRAS cells. Transduced cells were selected using puromycin (Sigma) for 2 days, then expanded for one passage, and injected into nude mice as described above. Real-time reverse transcription PCR (RT-PCR) for mouse *Tacc2, Tcf7l2*, and *Ablim1* used the following primers: mTacc2-F: CCT TTG AGA CCC CCG AGT, mTacc2-R: AAC ACC GCC GAG GAG GAG, mTcf7l2-F: CCC ACC ATG TCC ACC CAC, mTcf7l2-R: ATT TGT CCT ACG GTG CCG, mAblim1-F: ATT TAG CAG CCA TCC CCA, mAblim1-R: CGA TCC CGG ACA TCT TGA.

Sequencing of shRNAs from the *in vivo* screen

Tumors were necropsied from mice when they reached 2 cm in diameter or when the mice became moribund. The tumors were removed of normal skin and then flash frozen in liquid nitrogen. To sequence the shRNAs, two portions from opposite sides of each tumor were sampled. DNA was isolated using the DNEasy Kit (Qiagen) and PCR was carried out using pLKO-specific primers that flanked the hairpin: pLKO-seq-F, GAG GGC CTA TTT CCC ATG and pLKO-seq-R, GAT CTC TGC TGT CCC TGT A. PCR samples were run on agarose gels and visually confirmed to produce a single 490 bp band. Standard Sanger sequencing was then performed, with each tumor piece undergoing both forward and reverse sequencing. As a control, an shGFP tumor was also sequenced and confirmed.

In vitro invasion

Using the per-gene pooled four to five shRNAs isolated for the *in vivo* screen, cells from the iNRAS-463, iNRAS-650, and MMM-7.1 lines were infected in 24-well plates, one gene per well. An MOI of 2 was used to ensure 100% infection without drug selection. After 2 days of recovery from viral infection, cells were trypsinized for use in the invasion screen. The screen was carried out using 96-well Matrigel-coated invasion chambers (BD Biosciences) according to the manufacturer's instructions. Briefly, 1×10^4 cells per gene were plated per well, in triplicate, in serum-free RPMI and allowed to invade toward RPMI containing 10% FBS, over a period of 20 to 22 hours. Invaded cells were fixed and stained with Calcein AM, then quantified using a fluorescent plate reader. Simultaneously, an equal number of cells were seeded into cell culture wells containing RPMI, 1% FBS as loading controls. Invasion results were normalized against these loading controls. High-scoring genes were validated in 24-well invasion chambers (BD Biosciences), using 5×10^4 cells per well.

Human Ablim1 plasmids

A lentiviral-inducible shRNA against human Ablim1 in the pTRIPZ vector was purchased (Open Biosciences). Knockdown was confirmed by RT-PCR using the following primers: hAblim1-F, AAT GAG AAT GGA CCG AGG AG and hAblim1-R, CCA AAG ATT TCC CGA AAC AC. An Ablim1 overexpression construct was generated using Gateway cloning technology (Invitrogen) according to manufacturer's instructions. Briefly, a pENTR construct containing a full-length Ablim1 ORF (Origene, identical to NM_001003407) was cloned into a Gateway-compatible pHAGE vector (19) using LR Clonase II.

Results

Loss of large chromosomal regions is associated with decreased gene expression

We hypothesized that large regions of chromosomal loss might affect multiple tumor suppressor genes in melanoma. To narrow down regions of interest, we reanalyzed our previously published DNA copy number data from patient samples (6). Genomic nonnegative matrix factorization analysis had stratified the samples into three groups, of which the k1 and k2 populations had a significantly worse survival than k3 (6). We noted a strong enrichment in the k1 and k2 populations for broad regional losses of the 6q, 10, and 11q21-ter chromosomal regions (Supplementary Fig. S1). These three regions are also

Published OnlineFirst January 22, 2014; DOI: 10.1158/0008-5472.CAN-13-1446

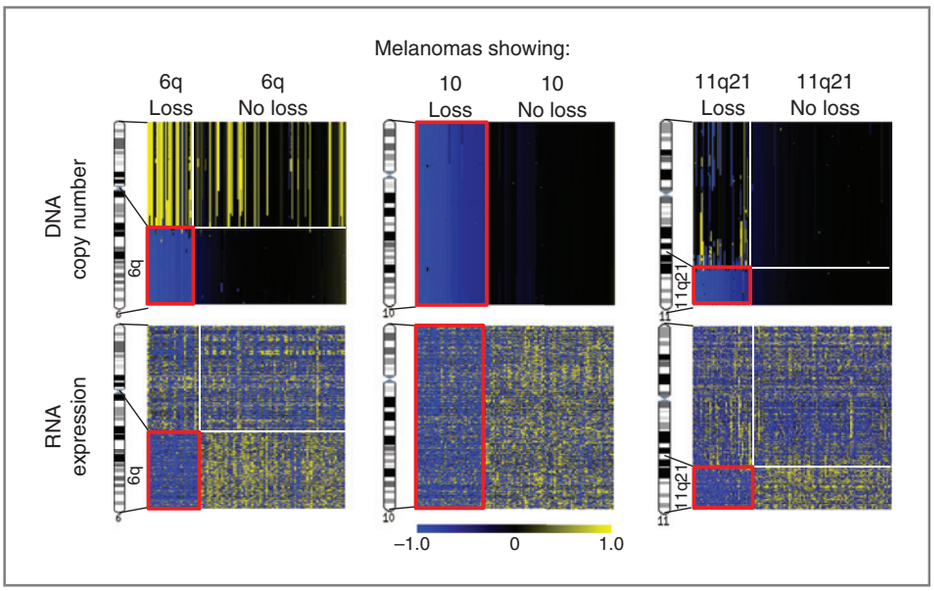

Figure 1. Genomic loss (red boxes, top) correlates with broadly decreased gene expression (red boxes, bottom) in the chromosome 6q, 10, and 11q21-ter regions. Each column is data from one melanoma, taken from TCGA. The color scale represents $\log_2$ data: for DNA, it indicates copy number and for RNA, it indicates median centering of expression levels across all samples. Only samples that showed either loss (<−0.5) or retention of two copies (>−0.2, <0.2) in each region are displayed (n = 135, 140, 150, respectively).

significantly lost in several other published melanoma datasets (7, 20, 21), including one in which poor survival was significantly correlated with loss of these three regions, among others (20). On the basis of our hypothesis, we focused on these regions as likely to be enriched for tumor suppressors.

We asked whether the loss of these regions perturbed the expression of the resident genes. We performed a cross-platform comparison of metastatic samples using matched DNA copy number and RNA expression data from The Cancer Genome Atlas (TCGA; Research Network, https://tcga-data.nci.nih.gov/tcga/dataAccessMatrix.htm, DOI # 2012-10-04). For each of the three regions, relevant samples were grouped into showing either chromosome loss (<−0.5, $\log_2$ value) or retention of two copies (>−0.2, <0.2). We identified a strong association between decreased copy number and region-wide decreased gene expression (Fig. 1). This is consistent with our hypothesis that broad DNA copy number losses can lead to the decreased gene expression of multiple putative tumor suppressors. To focus on a set of genes likely to have a functional tumor-suppressive role, we defined a set of 48 genes that are significantly downregulated in metastatic melanomas compared with either primary melanomas or benign nevi, by intersecting our previous data (6) with two other published microarray datasets (Supplementary Table S1 and Supplementary Fig. S2; refs. 14, 15).

Multiple genes on chromosome 10 are *in vivo* tumor growth suppressors

We next screened this list of 48 candidate tumor suppressors for *in vivo* tumor suppression activity via RNA interference (RNAi). First, we sought a well-characterized model system for screening these genes for tumor suppressor activity. We have previously described the iNRAS mouse model of melanoma (16), from which we have characterized multiple primary tumor-derived cell lines for their *in vivo* allograft growth. Two lines, iNRAS-485 and iNRAS-463, were selected to serve as the system for this functional genomic screen based on their relatively long latency (5–8 weeks). Four to five lentiviral shRNAs targeting each of the 48 candidate genes were pooled by genomic location. Cells were virally transduced at an MOI of 0.5 and injected into nude mice without any drug selection, to allow shRNA-bearing cells to compete with each other and with nontransduced cells.

In both of the iNRAS cell lines, tumors harboring shRNAs against genes in the 6q and 10, but not the 11q21-ter pools, exhibited increased growth rates compared with both a nontargeting shRNA control (shGFP) and the parental lines (Fig. 2A and B and Supplementary Fig. S3). In the iNRAS-463 cohort, chromosome 10 shRNAs were split into three equal groups based on chromosomal location (Supplementary Table S1). Only one of these three groups showed increased growth rate, group 10-3 (Fig. 2B).

If shRNA-mediated gene downregulation drives the observed increase in growth rates, we reasoned that these oncogenic shRNAs would be enriched in the individual resultant tumors. To identify such shRNAs, tumors exhibiting significantly increased growth in the iNRAS-485 line were sequenced by the Sanger-based method. In 24 of 36 tumors with high-quality sequencing reads, a single shRNA was identified (Fig. 2C), suggesting that such an shRNA was positively selected for driving the enhanced tumor growth. Importantly, all shRNAs were identified from their assigned pool, confirming that no cross-contamination had taken place. Of the 24 identified shRNAs, two genes were represented seven times

Published OnlineFirst January 22, 2014; DOI: 10.1158/0008-5472.CAN-13-1446

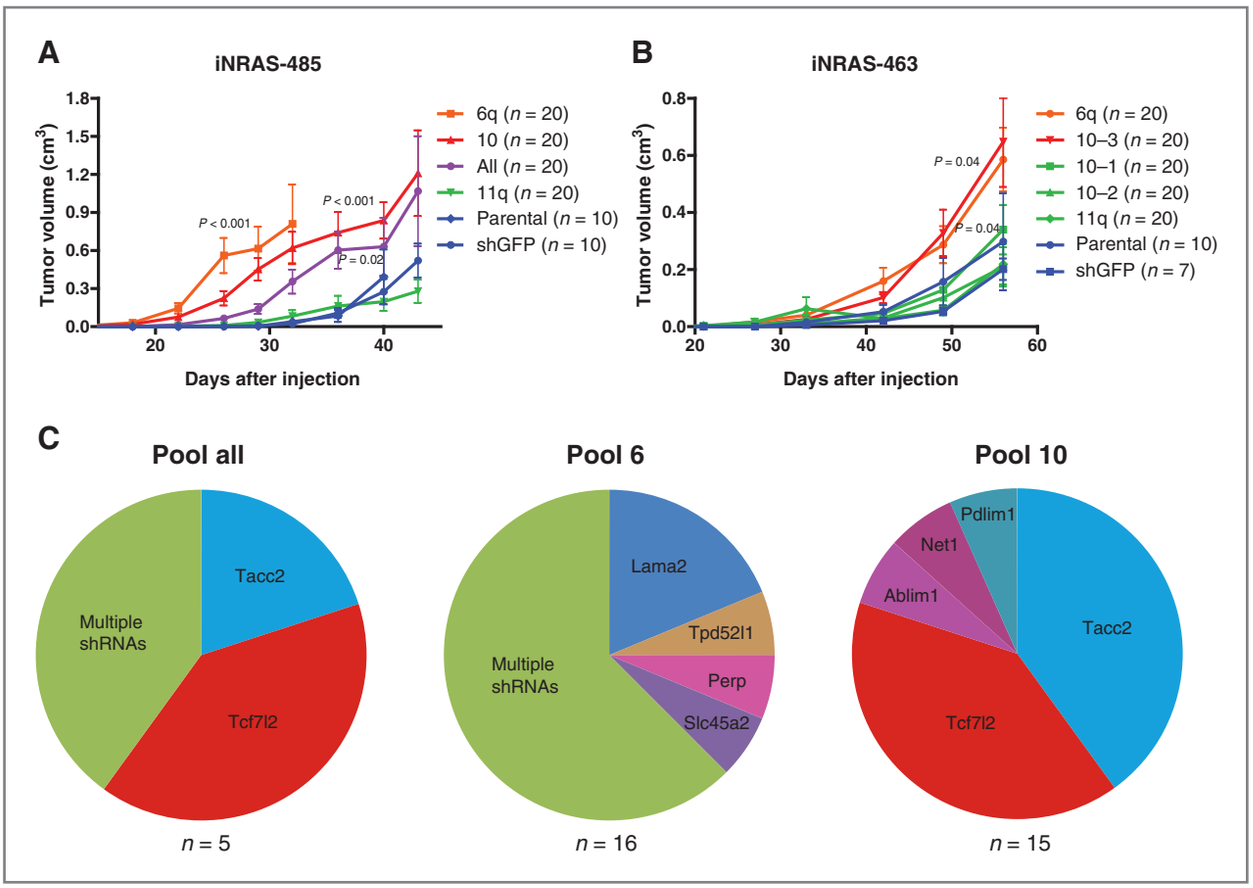

Figure 2. An *in vivo* shRNA screen for tumor suppressors. A, screening of 48 candidate genes for growth-suppressive effects in iNRAS-485 cell line allografts, showing average tumor volumes for intradermally injected cells. Genes are pooled by chromosome or all together and compared with parental and shGFP controls. B, screening of the same 48 genes in iNRAS-463 cell line allografts, showing average tumor volumes for intradermally injected cells. Genes are pooled by chromosome, with chromosome 10 broken into three smaller pools (see Supplementary Fig. S2). All *P* values are calculated using a two-tailed Student *t* test, comparing candidates to shGFP on the day of maximal tumor size. All error bars are SEM. C, results of shRNA sequencing from a total of 36 iNRAS-485 tumors showing enhanced growth and high-quality sequencing reads. All single shRNAs were cross-validated by sequencing two pieces from opposite sides of each tumor.

(enriched in seven independent tumors) each: *Tacc2* and *Tcf7l2* (Fig. 2C), both of which reside on chromosome 10.

We next performed secondary validation on all of the candidate tumor suppressors. First, to initially validate *Tacc2* and *Tcf7l2*, we pooled the five shRNAs per gene and generated stably knocked down cells. These cells formed tumors at significantly accelerated rates compared with controls (Fig. 3A). Other identified single shRNAs targeted the following genes: *Ablim1, Net1, Lama2, Pdlim1, Tpd52l1*, and *Perp* (Fig. 2C). The individual shRNAs sequenced from the initial screen were tested singly. Of these genes, only shRNAs targeting *Ablim1* and *Net1* significantly increased the tumor growth rate (Fig. 3B).

For tertiary validation, we selected our highest performing genes, *Tacc2, Tcf7l2*, and *Ablim1* for the testing of multiple single hairpins each to rule out off-target effects. For both *Tacc2* and *Tcf7l2*, we identified two shRNAs with strong knockdown efficiency, including the shRNAs identified by sequencing (shTacc2 #4 and shTcf7l2 #4). For both genes, these shRNAs each significantly enhanced the growth rate of the tumors (Fig. 4A and B). For *Ablim1*, we used all five available shRNAs because four of the five gave strong knockdown. Of these, three significantly decreased tumor latency in a third cell line, iNRAS-413 (Fig. 4C), and all three scoring hairpins knocked down *Ablim1* to a similar degree.

To address whether these colocalized tumor suppressors on chromosome 10 function cooperatively, we assessed the potency of *Tacc2* and *Tcf7l2* in combination and discovered that they did not significantly cooperate in affecting tumor latency or growth (Supplementary Fig. S3). These data suggest that the loss of these two genes may be phenotypically redundant or functionally parallel. Supporting these results is the observation that *Tacc2, Tcf7l2*, and *Ablim1* were all single-scoring genes within the 10-3 pool in the iNRAS-463 *in vivo* tumorigenesis screen (Fig. 2B and Supplementary Table S1).

Multiple genes on chromosome 10 are *in vitro* tumor invasion suppressors

As shown above, our *in vivo* functional genetic screen identified three suppressors of *in vivo* tumor growth, all

Published OnlineFirst January 22, 2014; DOI: 10.1158/0008-5472.CAN-13-1446

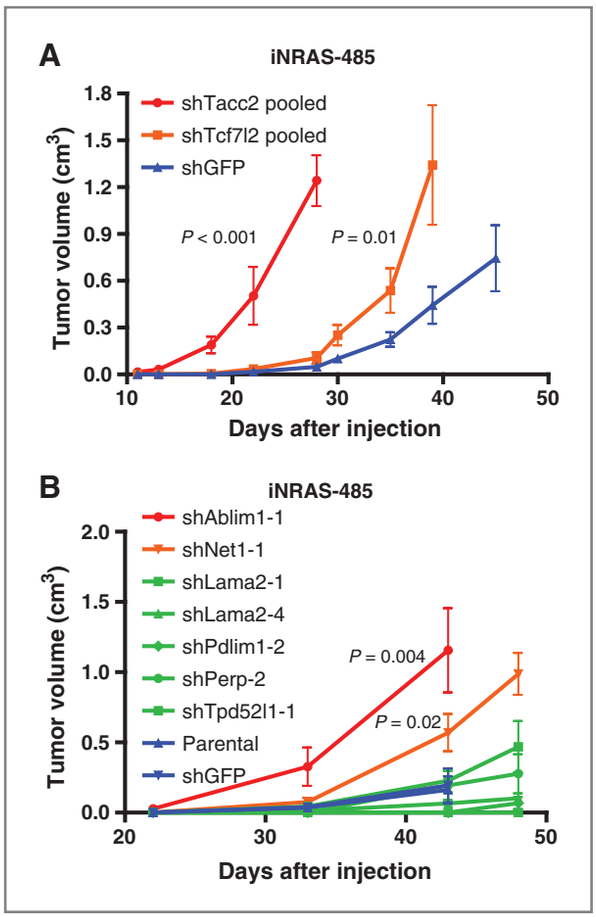

Figure 3. Secondary validation of candidate *in vivo* tumor suppressors. A, validation of Tacc2 and Tcf7l2 using five pooled shRNAs per gene. B, secondary screening of individual shRNAs for six candidate genes that were identified by sequencing in the primary screen. $N = 4$ per cohort except for shGFP ($n = 6$). All P values are calculated using a two-tailed Student t test, comparing candidates to shGFP on the day of maximal tumor size. All error bars are SEM.

resident genes on human chromosome 10q. Because the loss of chromosome 10 has been associated with metastatic potential in melanoma (6), we next sought to identify genes on this list of 48 that can suppress a different step in melanoma progression: invasion. Using the same model iNras* cell line system, we identified two lines with a low basal level of invasion through a Matrigel membrane: iNRAS-463 and iNRAS-650. To expand our assays, we generated an additional *in vitro* model by isolating ink/arf-null melanocytes and retrovirally adding human $BRAF^{V600E}$ and an shRNA against mouse *Pten*. This line, MMM-7.1, is nontransformed and was used at passages below six.

For the functional screen, four to five shRNAs were pooled per gene and each gene was tested individually using 96-well Boyden chamber assays. The results from one cell line are shown as a representative (Fig. 5A), demonstrating that the shGFP and parental controls fell roughly in the middle, as expected. Our analysis identified eight genes that, when knocked down, enhanced invasion in at least two of the three cell lines, including four that scored in all three (Fig. 5B). The top hit, *Acta2*, has been identified in a published *in vitro* shRNA invasion screen (22), supporting the validity of our results. Secondary validation was performed in 24-well Boyden chambers, confirming the anti-invasion effects of five of the eight candidate suppressors: *Ablim1, Acta2, C10orf57, Adra2a*, and *Ank3* (Fig. 5C), all of which are located on chromosome 10.

Functional analysis of Ablim1

As *Ablim1* was the only gene to score highly in both *in vivo* tumorigenesis and *in vitro* invasion assays, we selected it for further validation using human cell systems. First, we confirmed that *Ablim1* mRNA levels correlate significantly with the copy number status of chromosome 10 (Fig. 6A) in the TCGA patient dataset, consistent with it being one of the genes targeted by broad chromosomal loss. Next, using human cell lines selected for their baseline phenotypes (Supplementary Table S2), we showed that *Ablim1* knockdown resulted in a protumorigenesis phenotype manifested as a consistent, though modest, increase in tumor penetrance in two independent human cell lines, WM115 ($P = 0.1$) and 1205Lu ($P = 0.02$), by Kaplan–Meier analysis (Supplementary Fig. S4), although the rate of growth *in vivo* or *in vitro* was not enhanced (Supplementary Fig. S4). On the other hand, knockdown of *Ablim1* significantly enhanced the invasion of the poorly metastatic human WM115 cell line *in vitro* (Fig. 6B), whereas reciprocally, Ablim1 overexpression decreased invasion in the human SKMel28 and MUM2C cell lines compared with GFP (Fig. 6C). We next asked whether *Ablim1* can suppress invasion *in vivo*, in an experimental metastasis model. Indeed, overexpression of human *Ablim1* in the highly metastatic mouse cell line B16F10 resulted in a significant reduction in lung nodules after tail vein injection (Fig. 6D; $P = 5 \times 10^{-6}$). These data collectively validate *Ablim1* as a novel tumor suppressor in melanoma.

Discussion

In cancer, recurrent losses and gains of broad chromosome regions suggest that multiple genes in the same region may be cotargeted along with established tumor suppressors and oncogenes. Here, we provided functional evidence that in melanoma, recurrent loss of the entire chromosome 10 results in the repression of multiple tumor suppressors collectively regulating more than one step of cancer. A targeted RNAi screen of 48 genes, selected on the basis of expression levels in progressed human melanomas, revealed that knockdown of *Tacc2, Tcf7l2*, and Ablim1 enhances tumor growth *in vivo*, whereas knockdown of *Ablim1, Acta2*, and three other genes enhances invasion *in vitro*.

Consistent with our results, a recent study in melanoma also comparing DNA and RNA platforms identified 6q and 10q loss as significantly associated with ulceration, a negative prognostic indicator (21). Interestingly, their *in silico* analysis identified *Ablim1* as the only gene on 10q with a significant DNA and RNA correlation. We also note that all of our validated hits lie on 10q. Nevertheless, as our screen was purposefully targeted, it is likely that other genes resident on chromosome 10 may also be melanoma suppressors. Some

Published OnlineFirst January 22, 2014; DOI: 10.1158/0008-5472.CAN-13-1446

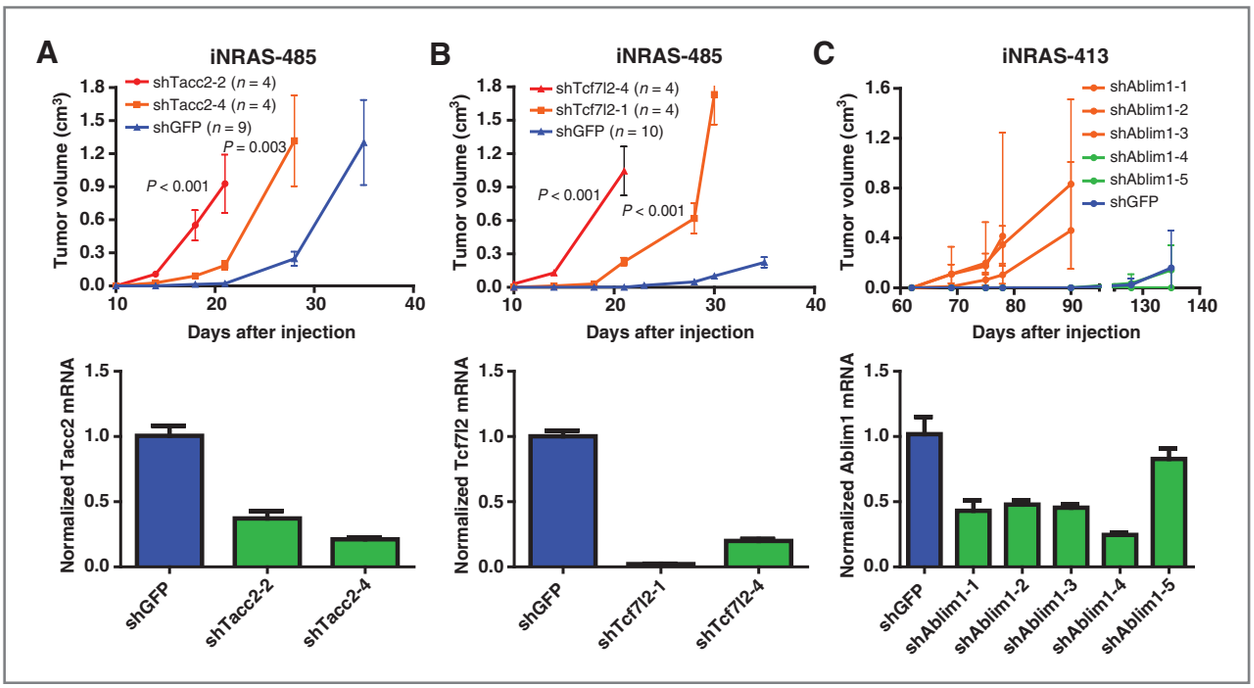

Figure 4. Tertiary validation of candidate *in vivo* tumor suppressors. A, top, validation of Tacc2 using two independent shRNAs. Bottom, RT-PCR quantitation of Tacc2 knockdown efficiency. B, top, validation of Tcf7l2 using two independent shRNAs. Bottom, RT-PCR quantitation of Tcf7l2 knockdown efficiency. C, top, validation of Ablim1 using five independent shRNAs. $N = 4$ per cohort. Bottom, RT-PCR quantitation of Ablim1 knockdown efficiency. All P values are calculated using a two-tailed Student t test, comparing candidates to shGFP on the day of maximal tumor size. All error bars are SEM.

possibilities include *CUL2* and *KLF6*, which have been proposed as candidate targets in melanoma based on *in silico* analyses (7).

Consistent with published data, all four of our top hits have previously been described as tumor suppressors. *Tcf7l2* was a top hit in an *in vitro* shRNA screen in colon cancer (23) and has

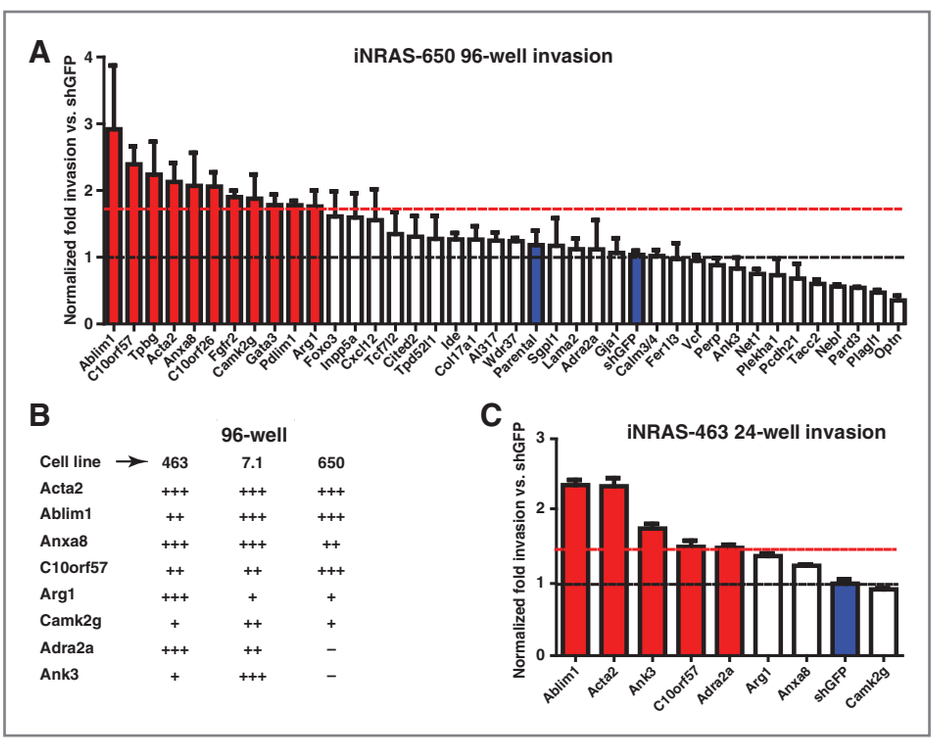

Figure 5. An *in vitro* invasion screen. A, representative results from the iNRAS-650 cell line. Parental and shGFP controls are highlighted in blue. Significant genes are highlighted in red, defined as one SD above the control (dashed red line). B, summary of top hits from the screen. To generate a normalized comparison between the three cell lines, positively scoring genes were categorized as having a nonsignificant (–), weak (+), medium (++), or strong (+++) effect versus shGFP, and were significant in at least two cell lines. C, validation of the top hits in 24-well invasion chambers. All error bars are SEM.

Published OnlineFirst January 22, 2014; DOI: 10.1158/0008-5472.CAN-13-1446

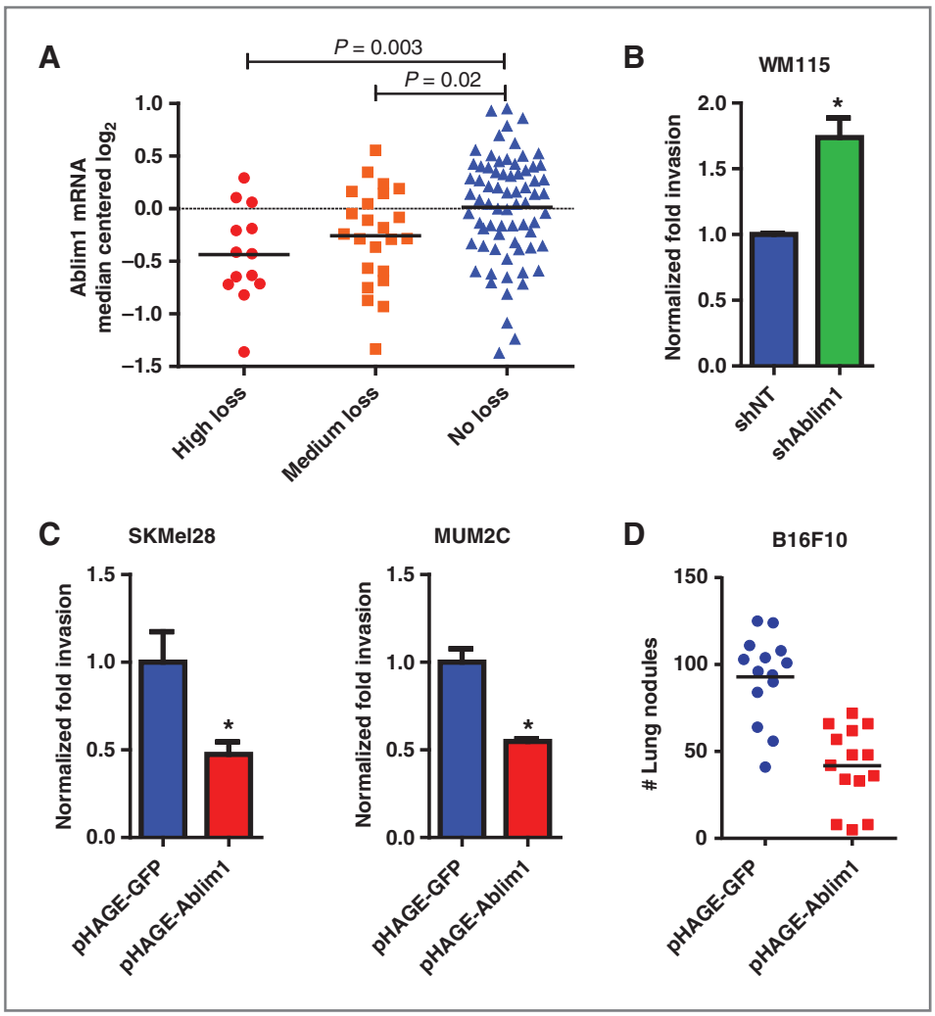

Figure 6. Ablim1 suppresses invasion. A, Ablim1 expression levels in the TCGA dataset correlate with copy number loss of chromosome 10: high (<−0.8) or medium (>−0.7, <−0.5) loss, or retention of two copies (>−0.2, <0.2). B, Ablim1 knockdown enhances invasion in WM115 cells. pTRIPZ is a doxycycline-inducible vector, and both the nontargeting shNT and shAblim1 cells were treated with doxycycline. *, $P < 0.05$, Student *t* test. C, Ablim1 overexpression inhibits invasion in SKMel28 and MUM2C cells. All error bars are SEM. D, Ablim1 overexpression inhibits lung nodule formation after tail vein injection of B16F10 cells. $n = 14$ each cohort.

been validated as an *in vivo* tumor suppressor using a mouse knockout model (24). *Tacc2* was initially described as a breast tumor suppressor (25), and has since been described as either a tumor suppressor or oncogene (26, 27), depending on the cell type context. *Acta2* was a top hit in another melanoma RNAi screen, where knockdown strongly enhanced invasion through a three-dimensional collagen/Matrigel plug (22). Finally, *Ablim1* was a significant hit in an *in vivo* retrotranspon mutagenesis screen, where multiple inactivating insertions were documented in tumors of p19- and p53-deficient mice (28). Interestingly, reanalysis of published iNRAS mouse microarray data (16) found that NRAS signaling represses the expression of *Ablim1, Acta2*, and *Tcf7l2* (Supplementary Fig. S5). Furthermore, in the TCGA metastatic sample dataset, samples with BRAF or NRAS hotspot mutations, but not NF1 mutations, were significantly enriched for chromosome 10 loss (Supplementary Fig. S5). These *in silico* findings suggest that chromosome 10 loss and canonical mitogen-activated protein kinase signaling may corepress these tumor suppressors.

Although we validated multiple hits on chromosome 10, shRNAs on chromosome 6 (*Lama2, Perp, Tpd52l1, Slc45a2*) failed to validate as single shRNAs in our secondary screens. One possibility is that these shRNAs were false positives. Another possibility is that chromosome 6 shRNAs require cooperation to affect the phenotype. Indeed, the results of our shRNA sequencing show that 63% (10/16) of the chromosome 6 tumors harbored multiple shRNAs, in contrast with zero of 15 of the chromosome 10 tumors (Fig. 2C). This suggests that, unlike chromosome 10, the majority of chromosome 6 tumors may have required multiple coexisting shRNAs to enhance tumor growth. Further study will be required to deconvolute these shRNA pools and to test their combinations. Finally, none of the chromosome 11 shRNAs scored in either of our primary screens, suggesting that other genes in the region may be the true targets of the recurrent loss.

In summary, our study demonstrates that loss of chromosome 10 in melanoma likely targets more than just the *PTEN* tumor suppressor and that these other genes may collectively or redundantly act at more than one step in progression. This provides functional data in support of the thesis that broad regional loss of chromosomes is one mechanism to target multiple tumor suppressors in cancers.

Published OnlineFirst January 22, 2014; DOI: 10.1158/0008-5472.CAN-13-1446

Disclosure of Potential Conflicts of Interest

No potential conflicts of interest were disclosed.

Authors' Contributions

Conception and design: L.N. Kwong, L. Chin
Analysis and interpretation of data (e.g., statistical analysis, biostatistics, computational analysis): L.N. Kwong, L. Chin
Writing, review, and/or revision of the manuscript: L.N. Kwong, L. Chin
Study supervision: L.N. Kwong, L. Chin

Acknowledgments

The authors thank Dr. W. Hahn for the shRNA clones, members of the laboratory for their insightful discussions, particularly S. Quayle and N. Sharma, S. Colla for the pHAGE backbone, C. Bristow for TCGA data validation, and R. Kwong for manuscript proofreading.

Grant Support

This work was supported by Postdoctoral Fellowship 117842-PF-09-261-01-TBG from the American Cancer Society (L.N. Kwong), Abby S. and Howard P. Milstein 2009 Innovation Award for Melanoma and Skin Cancer Research, and Cancer Prevention Research Institute of Texas Scholar in Cancer Research (L. Chin).

The costs of publication of this article were defrayed in part by the payment of page charges. This article must therefore be hereby marked *advertisement* in accordance with 18 U.S.C. Section 1734 solely to indicate this fact.

Received May 22, 2013; revised November 23, 2013; accepted December 16, 2013; published OnlineFirst January 22, 2014.

References

1. Chin L, Hahn WC, Getz G, Meyerson M. Making sense of cancer genomic data. Genes Dev 2011;25:534–55.
2. Yates LR, Campbell PJ. Evolution of the cancer genome. Nat Rev Genet 2012;13:795–806.
3. Ghosh P, Chin L. Genetics and genomics of melanoma. Expert Rev Dermatol 2009;4:131.
4. Shi H, Moriceau G, Kong X, Lee MK, Lee H, Koya RC, et al. Melanoma whole-exome sequencing identifies V600EB-RAF amplification-mediated acquired B-RAF inhibitor resistance. Nat Commun 2012;3:724.
5. Vízkeleti L, Ecsedi S, Rákosy Z, Orosz A, Lázár V, Emri G, et al. The role of CCND1 alterations during the progression of cutaneous malignant melanoma. Tumor Biol 2012;33:2189–99.
6. Kabbarah O, Nogueira C, Feng B, Nazarian RM, Bosenberg M, Wu M, et al. Integrative genome comparison of primary and metastatic melanomas. PLoS ONE 2010;5:e10770.
7. Lin WM, Baker AC, Beroukhim R, Winckler W, Feng W, Marmion JM, et al. Modeling genomic diversity and tumor dependency in malignant melanoma. Cancer Res 2008;68:664–73.
8. Solimini NL, Xu Q, Mermel CH, Liang AC, Schlabach MR, Luo J, et al. Recurrent hemizygous deletions in cancers may optimize proliferative potential. Science 2012;337:104–9.
9. Xue W, Kitzing T, Roessler S, Zuber J, Krasnitz A, Schultz N, et al. A cluster of cooperating tumor-suppressor gene candidates in chromosomal deletions. Proc Natl Acad Sci 2012;109:8212–7.
10. Cowan J, Francke U. Cytogenetic analysis in melanoma and nevi. In: Nathanson L, editor. Melanoma Research: Genetics, Growth Factors, Metastases, and Antigens: Springer US; 1991. p. 3–16.
11. Guldberg P, thor Straten P, Birck A, Ahrenkiel V, Kirkin AF, Zeuthen J. Disruption of the MMAC1/PTEN gene by deletion or mutation is a frequent event in malignant melanoma. Cancer Res 1997;57:3660–3.
12. Robertson GP, Furnari FB, Miele ME, Glendening MJ, Welch DR, Fountain JW, et al. In vitro loss of heterozygosity targets the PTEN/MMAC1 gene in melanoma. Proc Natl Acad Sci 1998;95:9418–23.
13. McClintick J, Edenberg H. Effects of filtering by Present call on analysis of microarray experiments. BMC Bioinformatics 2006;7:49.
14. Talantov D, Mazumder A, Yu JX, Briggs T, Jiang Y, Backus J, et al. Novel genes associated with malignant melanoma but not benign melanocytic lesions. Clin Cancer Res 2005;11:7234–42.
15. Riker A, Enkemann S, Fodstad O, Liu S, Ren S, Morris C, et al. The gene expression profiles of primary and metastatic melanoma yields a transition point of tumor progression and metastasis. BMC Med Genomics 2008;1:13.
16. Kwong LN, Costello JC, Liu H, Jiang S, Helms TL, Langsdorf AE, et al. Oncogenic NRAS signaling differentially regulates survival and proliferation in melanoma. Nat Med 2012;18:1503–10.
17. Kim M, Gans JD, Nogueira C, Wang A, Paik JH, Feng B, et al. Comparative oncogenomics identifies NEDD9 as a melanoma metastasis gene. Cell 2006;125:1269–81.
18. Nogueira C, Kim KH, Sung H, Paraiso KHT, Dannenberg JH, Bosenberg M, et al. Cooperative interactions of PTEN deficiency and RAS activation in melanoma metastasis. Oncogene 2010;29:6222–32.
19. Muller FL, Colla S, Aquilanti E, Manzo VE, Genovese G, Lee J, et al. Passenger deletions generate therapeutic vulnerabilities in cancer. Nature 2012;488:337–42.
20. Hirsch D, Kemmerling R, Davis S, Camps J, Meltzer PS, Ried T, et al. Chromothripsis and focal copy number alterations determine poor outcome in malignant melanoma. Cancer Res 2012;73:1454–60.
21. Rakosy Z, Ecsedi S, Toth R, Vizkeleti L, Herandez-Vargas H, Lazar V, et al. Integrative genomics identifies gene signature associated with melanoma ulceration. PLoS ONE 2013;8:e54958.
22. Gobeil S, Zhu X, Doillon CJ, Green MR. A genome-wide shRNA screen identifies GAS1 as a novel melanoma metastasis suppressor gene. Genes Dev 2008;22:2932–40.
23. Tang W, Dodge M, Gundapaneni D, Michnoff C, Roth M, Lum L. A genome-wide RNAi screen for Wnt/β-catenin pathway components identifies unexpected roles for TCF transcription factors in cancer. Proc Natl Acad Sci 2008;105:9697–702.
24. Angus-Hill ML, Elbert KM, Hidalgo J, Capecchi MR. T-cell factor 4 functions as a tumor suppressor whose disruption modulates colon cell proliferation and tumorigenesis. Proc Natl Acad Sci 2011;108:4914–9.
25. Chen H-M, Schmeichel KL, Mian IS, Lelièvre S, Petersen OW, Bissell MJ. AZU-1: a candidate breast tumor suppressor and biomarker for tumor progression. Mol Biol Cell 2000;11:1357–67.
26. Lauffart B, Gangisetty O, Still IH. Molecular cloning, genomic structure and interactions of the putative breast tumor suppressor TACC2. Genomics 2003;81:192–201.
27. Takayama K, Horie-Inoue K, Suzuki T, Urano T, Ikeda K, Fujimura T, et al. TACC2 is an androgen-responsive cell cycle regulator promoting androgen-mediated and castration-resistant growth of prostate cancer. Mol Endocrinol 2012;26:748–61.
28. Uren AG, Kool J, Matentzoglu K, de Ridder J, Mattison J, van Uitert M, et al. Large-scale mutagenesis in p19ARF- and p53-deficient mice identifies cancer genes and their collaborative networks. Cell 2008;133:727–41.

Cancer Research
The Journal of Cancer Research (1916–1930) | The American Journal of Cancer (1931–1940)

AACR American Association for Cancer Research

Chromosome 10, Frequently Lost in Human Melanoma, Encodes Multiple Tumor-Suppressive Functions

Lawrence N. Kwong and Lynda Chin

Cancer Res 2014;74:1814-1821. Published OnlineFirst January 22, 2014.